Hair Growth Cycle Is Arrested in SCD1 Deficiency by Impaired Wnt3a-Palmitoleoylation and Retrieved by the Artificial Lipid Barrier

Wilhelm Stoffel[1,2,3], Inga Schmidt-Soltau[1], Britta Jenke[1], Erika Binczek[1] and Ina Hammels[1,2]

Stearoyl-CoA desaturase 1 (SCD1) is the dominant member of the SCD-isozyme family, regarded as a major regulator of lipid and energy metabolism in liver and adipose tissue. SCD1 deficiency impairs the desaturation of de novo-synthesized palmitoyl- and stearoyl-CoA to palmitoleoyl- and oleoyl-CoA. *Scd1*$^{-/-}$ mice develop metabolic waste syndrome and skin lesions: epidermal barrier disruption, alopecia, and degeneration of sebaceous glands. The unifying molecular link between the two divergent traits remains incompletely understood. Here we show the absence of palmitoleic acid (9Z-16:1) in the lipidome of the *scd1-null* mouse, which prohibits posttranslational O-palmitoleoylation of Wnt3a protein, essential for Wnt3a/ß-catenin signaling in stem cell lineage decision in development of the epidermal barrier, hair growth cycle, and sebaceous glands. Substitution of the disrupted epidermal lipid barrier by an inert hydrocarbon coat prevents excessive transepidermal water loss, normalizes thermogenesis and metabolic parameters, and surprisingly leads to the activation of hair bulge progenitor cells and reprograming of a regular hair growth cycle and development of a regular fur in *scd1*$^{-/-}$ mice. Progenitor sebocytes are not activated. Independent of age, application or removal of the artificial lipid barrier allows the reversible telogen-anagen reentry and exit of the hair growth cycle.

Journal of Investigative Dermatology (2017) **137,** 1424–1433; doi:10.1016/j.jid.2017.02.973

INTRODUCTION

Stearoyl-CoA-desaturases (SCD isozymes) catalyse the stereo- and position-specific Δ9-desaturation of de novo-synthesized palmitoyl- and stearoyl-CoA to Δ9-palmitoleoyl- and oleoyl-CoA. *Scd1*, the main SCD isozyme, is expressed constitutively in adipose tissue and inducible in liver, SCD2, constitutively in brain tissue and inducible in kidney, lung, spleen, skin, and adipose tissue, but absent in liver. Notably, SCD3 expression is restricted to sebaceous glands of skin, the Harderian and preputial gland and developing adipocytes (Miyazaki et al., 2006; Zheng et al., 2001). Targeted deletion of *scd1* expression in the mouse causes a bipartite phenotype, a severe metabolic waste syndrome (anti-obesity), and disruption of the epidermal barrier function, alopecia, and degeneration of sebaceous glands (Binczek et al., 2007; Miyazaki et al., 2001).

Molecular mechanisms underlying the *scd1*$^{-/-}$ phenotype are at present incompletely understood and controversially discussed. SCD1 is regarded as an important regulator of lipid metabolism in liver and muscle. The metabolic waste syndrome has been interpreted by suppression of genes, regulating lipogenesis and upregulation of gene expression of enzymes in lipid catabolism, including a metabolic response of SCD1 to leptin, the hormone, secreted by adipose tissue (Cohen et al., 2002; Ntambi and Miyazaki, 2003).

Our previous studies unveiled the disruption of the epidermal multilamellar intercellular lipid barrier in the stratum corneum in SCD1 deficiency as the primary causal nexus between the anti-obesity syndrome and severe skin phenotype. Loss of barrier properties caused uncontrolled transepidermal water loss (TEWL) and heat dissipation, excessive thermogenesis, and imbalance of systemic energy homeostasis (Binczek et al., 2007). Support of this concept comes from a subsequent study in a skin-specific *scd1null*-mouse mutant (Sampath et al., 2009).

Exploring the molecular basis of the intricate *scd1*$^{-/-}$ phenotype we analyzed the lipidome of skin, mesenterial and subcutaneous white adipose tissue (WAT) and brown adipose tissue, liver, and brain of control and *scd1*$^{-/-}$ mice, to pinpoint critical alterations of their lipidomes.

Here, we report the systemic absence of palmitoleic acid (9Z-16:1) in the *scd1*$^{-/-}$ mouse and provide, to our knowledge, a previously unreported molecular aspect of the role of SCD1. De novo-synthesized palmitoyl-CoA is not desaturated to palmitoleoyl-CoA in the SCD1-deficient mouse unlike stearoyl-CoA, which, as a substrate of the remaining SCD isozymes, becomes compensatory desaturated to oleoyl-CoA in the *scd1*$^{-/-}$ mouse.

Wnt3a/ß-catenin signaling has emerged as a dominant canonical pathway in early cell lineage decision and

[1]*Laboratory of Molecular Neurosciences, Institute of Biochemistry, University of Cologne, Cologne, Germany;* [2]*CMMC (Center of Molecular Medicine), University of Cologne, Cologne, Germany; and* [3]*CECAD (Cluster of Excellence: Cellular Stress Responses in Aging-Associated Diseases), University of Cologne, Cologne, Germany*

Correspondence: Wilhelm Stoffel, Laboratory of Molecular Neuroscience, Institute of Biochemistry, University of Cologne, Joseph-Stelzmann-Straße 52, 50931 Cologne, Germany. E-mail: wilhelm.stoffel@uni-koeln.de

Abbreviations: IFE, interfollicular epidermis; SCD1, stearoyl-CoA desaturase 1; TEWL, transepidermal water loss; WAT, white adipose tissue

Received 3 November 2016; revised 9 January 2017; accepted 7 February 2017; accepted manuscript published online 1 March 2017; corrected proof published online 17 May 2017

controlling skin barrier homeostasis, hair growth cycle, and the function of sebaceous glands (Andl et al., 2002; DasGupta and Fuchs, 1999; Huelsken and Birchmeier, 2001; Lowry et al., 2005); for a review, see Lim and Nusse (2013).

Wnt3a is activated by glycosylation and lipidation (Nusse, 2003; Takada et al., 2006; Willert et al., 2003). O-Palmitoleoylation (9Z-16:1) of Wnt3a has been discovered as essential posttranslational lipidation, essential for intracellular transport, secretion, and receptor-mediated activation of the Wnt3a/ß-catenin signaling pathway (Takada et al., 2006). This modification is catalyzed by membrane-bound O-acyltransferase (Hofmann, 2000) in the endoplasmic reticulum (Zhai et al., 2004).

The absence of 9Z-16:1 in the *scd1*$^{-/-}$ mouse precludes this crucial hydrophobic modification of Wnt.

In further elaborating the mechanism underlying the bipartite *scd1*$^{-/-}$ phenotype, we suppressed the severe water loss through the disrupted epidermal multilamellar intercellular lipid barrier (TEWL) by an inert continuous whole-body hydrocarbon coat, a mimicry of the epidermal lipid barrier (*scd1*$^{-/-c}$). This artificial barrier reconstituted the physical properties of the disrupted epidermal barrier and normalized excessive TEWL, heat loss, thermogenesis, and metabolic parameters of the *scd1*$^{-/-}$ mouse.

Surprisingly, progenitor cells were activated selectively in the hair bulge and interfollicular epidermis (IFE). A regular hair growth cycle and morphology, and fur were reconstituted and alopecia was abolished in *scd1*$^{-/-}$ mice. Progenitor sebocytes were not activated.

This intervention allowed reversible activation or suppression of the hair growth cycle ad libitum during the life span of the *scd1*$^{-/-}$ mouse.

RESULTS

9Z-16:1 is missing in the *scd1null* mouse

Three mouse lines were used in this study: control, *scd1*$^{-/-}$, and *scd1*$^{-/-c}$ mice. Classes of neutral, phospho- , and sphingolipids in the lipidome of extraneuronal tissues, skin including protein-bound ω-hydroxylated fatty acid substituted ceramides, mesenterial, and subcutaneous white adipose tissue (mWAT and sWAT), liver, brain, and brown adipose tissue in adult control, *scd1*$^{-/-}$, and *scd1*$^{-/-c}$ mice, were separated by high-performance thin-layer chromatography for quantitative tandem mass spectrometry and their fatty acid substitutes identified and quantitated as methyl esters by combined gas chromatography/mass spectrometry analysis. We observed a rapid decrease of 9Z-16:1 during postnatal development, from 6% of total fatty acids to 0.5% at p12 and the absence at p21 in the lipidomes of all extraneuronal tissues of *scd1*$^{-/-}$ mice investigated (Figure 1a–f and Supplementary Figure S1a–c online).

Of note is the low concentration of 9Z-16:1 in control, but the absence in *scd1*$^{-/-}$ mWAT (3%), sWAT (2%), and brown adipose tissue (2%) (Figure 1f). Trace amounts of 16:1 in the liver at p21 and p35 were identified as 16:1^{7} by gas chromatography/mass spectrometry of its dimethyl oxazoline derivative (M^{+} 307) (Archives of Mass-Spectra, AOCS Lipid Library). 7Z-16:1 originates from 9Z-18:1 by one turn of ß-oxidation.

The absence of 16:0-CoA desaturation in *scd1*$^{-/-}$ mice was further proven by the desaturase assay, using the liver microsomal fraction as an enzyme source and [1-^{14}C] 16:0-CoA as a substrate. Reaction products were separated by argentation-thin-layer chromatography analysis, visualized and quantified by autoradiography in respective adsorbent bands (Supplementary Figure S1d).

Real-time PCR of cRNAs of the skin of control, *scd1*$^{-/-}$, and *scd1*$^{-/-c}$ mice, using oligonucleotide primer pairs, listed in Supplementary Table S1 (online), revealed complete suppression of *scd1* and *scd3* and minor induction of *scd2* expression. *Scd3* is expressed transiently only in sebocytes of mice (Miyazaki et al., 2006). Ceramide synthases CERS1 and CERS5, which preferentially transfer stearoyl and palmitoyl residues to sphingosine and dihydrosphingosine, are strongly downregulated in *scd1*$^{-/-}$ mice (Figure 1g).

Absence of palmitoleic acid perturbs Wnt3a/ß-catenin signaling in the *scd1null* mouse skin

Posttranslational O-palmitoleoylation (9Z-16:1) of Wnt3a protein is essential for the activation of the Wnt/ß-catenin signaling pathway (Takada et al., 2006; Willert et al., 2003). 16:1 has been identified as a substrate of endoplasmic reticulum membrane-bound O-acyltransferase for posttranslational Wnt-acylation into the hydrophobic secretion-competent signaling molecule, essential for transport, raft targeting, and secretion. The systemic 16:1 deficiency, reported here, prohibits this posttranslational modification essential for canonical Wnt3a-ß-catenin activation in the *scd1*$^{-/-}$ mouse.

We next studied the impact of 16:1 deficiency on the expression of the Wnt3a/ß-catenin system. Real-time PCR analysis of *wnt3a, 4, 10, porc, ß-catenin* and downstream *lef1* of the skin of control, *scd1*$^{-/-}$, and *scd1*$^{-/-c}$ mice indicated significant (3-fold) downregulation of *wnt3a* expression in the skin of *scd1*$^{-/-}$ mice. ß-Catenin expression in the control, *scd1*$^{-/-}$, and *scd1*$^{-/-c}$ skin remained unchanged, and *porc* expression in the skin of *scd1*$^{-/-}$ and *scd1*$^{-/-c}$ mice was elevated 3–4 times and of *lef1* approximately 10 times (Figure 2a).

Anti-Scd1 did not detect any Scd1 immunoreactive peptides in *scd1*$^{-/-}$ and *scd1*$^{-/-c}$ mice (Figure 2b). Complementary to the transcriptional expression results, western blot analysis revealed reduced Wnt3a and ß-catenin but elevated Lef1 concentrations in *scd1*$^{-/-}$ skin lysates. The artificial barrier had no impact on transcription and translation of genes of the Wnt3a-ß-catenin-Lef1 signal system (Figure 2a and c–e). *Lef1* remained activated independent of the suppression of *wnt3a* transcription and missing O-palmitoleoylation for Wnt3a activation in IFE, outer and inner root sheath nuclear localization (Figure 2h and j). Immunohistochemistry using anti-ß-catenin antibodies confirms the insignificantly changed expression on the transcriptional and translational level (Figure 2i).

Furthermore, we have quantitated gene expression on the translational level for key markers of pathways, bone morphogenic protein inhibitors active in (i) telogen, (ii) Noggin and Wnt in the telogen-anagen transition, and (iii) Shh in early anagen (Figure 2f and g) (Hsu et al., 2014). The expression of these marker genes is strongly

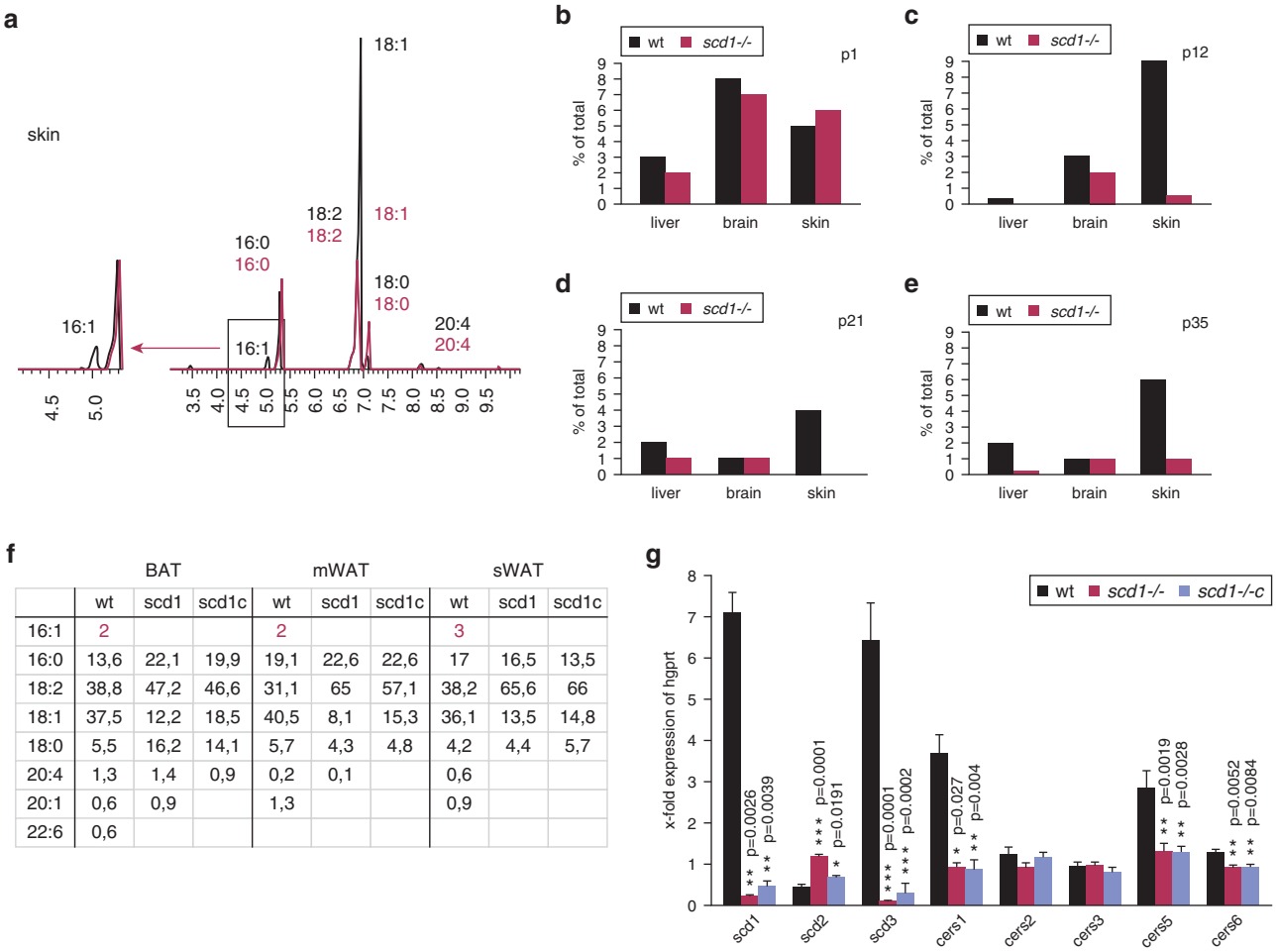

	BAT			mWAT			sWAT		
	wt	scd1	scd1c	wt	scd1	scd1c	wt	scd1	scd1c
16:1	2			2			3		
16:0	13,6	22,1	19,9	19,1	22,6	22,6	17	16,5	13,5
18:2	38,8	47,2	46,6	31,1	65	57,1	38,2	65,6	66
18:1	37,5	12,2	18,5	40,5	8,1	15,3	36,1	13,5	14,8
18:0	5,5	16,2	14,1	5,7	4,3	4,8	4,2	4,4	5,7
20:4	1,3	1,4	0,9	0,2	0,1		0,6		
20:1	0,6	0,9		1,3			0,9		
22:6	0,6								

Figure 1. Systemic loss of 16:1 in weaning *scd1*$^{-/-}$ mice. GC/MS of fatty acid substitutes of ester and amide lipids of skin revealed the absence of 9Z-16:1 in *scd1*$^{-/-}$ mice. (**a**) GC/MS tracings of fatty acid methyl esters of adult control (black) and *scd1*$^{-/-}$ mice skin (red). The bar diagrams of 9Z-16:1 concentration (mole % of total fatty acids) of control (black bars) and *scd1*$^{-/-}$ (red bars) of liver, brain, and skin at (**b**) p1, (**c**) p12, (**d**) p21, and (**e**) p35 mice. (**f**) Fatty acid composition of total lipids of BAT, mWAT, and sWAT (mole %). (**g**) Real-time PCR of *scd1, 2, 3* and ceramide *synthases (cers) 1, 2, 3, 5,* and *6*. Mean ± SD. BAT, brown adipose tissue; GC/MS, gas chromatography/mass spectrometry; SD, standard deviation; WAT, white adipose tissue; wt, wild-type.

downregulated in the *scd1*$^{-/-}$ and *scd1*$^{-/-c}$ skin and not rescued by the artificial lipid coat, as shown in Figure 2.

Artificial physical barrier reconstituted key functions of the disrupted *scd1*$^{-/-}$ epidermal lipid barrier and reprograms the hair cycle of adult *scd1*$^{-/-}$ mice

Experiments subsequent to our previous observation of the rescue of the malfunctioning epidermal lipid barrier in the SCD1-deficient mouse by a whole-body continuous inert paraffin coat further support our concept of the causal nexus between the severe waste of energy and the compensatory hypermetabolism and disrupted thermogenesis (Binczek et al., 2007).

The hair growth cycle in *scd1*$^{-/-}$ mice persists in telogen (Binczek et al., 2007; Miyazaki et al., 2001; Sundberg et al., 2000). The application of the artificial lipid barrier, most surprisingly, induced the anagen phase and led to the recapitulation of the embryonic hair growth cycle within a 3-week intervention (Figure 3b). The absence of vibrissae in *scd1*$^{-/-}$ mice is shown in Figure 3c. Cyclic application and removal of the artificial physical barrier initiated or interrupted the hair growth cycle in adult male and female *scd1*$^{-/-}$ mice. Likewise, melanocytes regenerated from the new hair follicle bulb, but not sebaceous glands.

We compared the hair morphology of isolated hair, hair shafts, and hair bulbs of control, scd1$^{-/-}$, and *scd1*$^{-/-c}$ mice at days 5, 15, and 25 after initiation of topical application (Figure 3e–i) and observed the same morphology in control and coated *scd1*$^{-/-}$ mice.

We have carried out follow-up TEWL measurements of control, *scd1*$^{-/-}$, and *scd1*$^{-/-c}$ mice over a period of 1 month (Figure 3j). The decrease of TEWL of *scd1*$^{-/-c}$ reaches the TEWL values of control mice within 5–8 days after the first topical application and remains constantly low during the treatment. This suggests semipermeability, similar to the normal stratum corneum. The impact of the artificial barrier on the general metabolism has been extensively described previously (Binczek et al., 2007).

Regular patterned expression of hair follicle markers in the *scd1*$^{-/-c}$ skin

De novo synthesis of hair follicles in the *scd1*$^{-/-c}$ skin progressed through anagen, catagen, and telogen of the growth cycle, and produced a regular hair shaft.

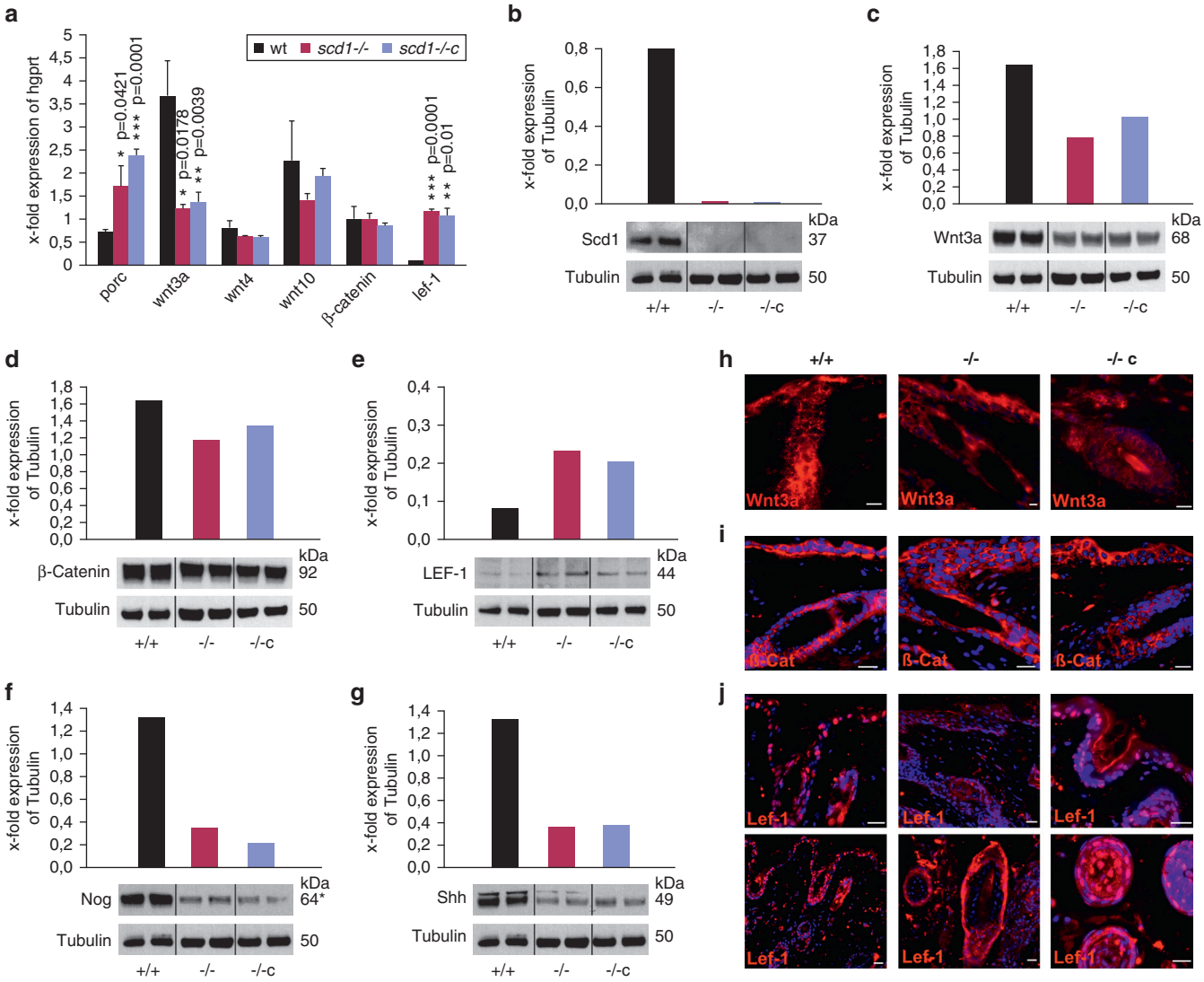

Figure 2. Quantitation of gene expression of Wnt3a/ß-catenin signaling pathway proteins. (**a**) Real-time PCR of *porcupine (porc), wnt3a, 4* and *10, ß-catenin* and *lef1* in the control, $scd1^{-/-}$, and $scd1^{-/-c}$ skin. RNA was isolated from the skin of five 2-month-old male mice. Mean ± SD densitometry of western blot analyses using: (**b**) anti-Scd1, (**c**) anti-Wnt3a, (**d**) anti-ß-catenin, (**e**) anti-Lef1, (**f**) anti-Nog (Noggin), *dimer, and (**g**) anti-Shh (Sonic Hedgehog) antibodies. IHC of the control, $scd1^{-/-}$, and $scd1^{-/-c}$ skin, using (**h**) anti-Wnt3a antibodies, (**i**) anti-ß-catenin, and (**j**) anti-Lef1 antibodies. Scale bar = 20 μm. IHC, immunohistochemistry; SD, standard deviation; wt, wild-type.

The sequence of developmental processes during lineage commitment of undifferentiated stem and progenitor cells in the skin commences with the expansion of a population of highly proliferative cells and their subsequent terminal differentiation of the epidermis including epidermal appendages, hair follicle, and sebaceous gland in the mouse skin (Alonso and Fuchs, 2003).

These stages were well delineated in the activated growth cycle of the $scd1^{-/-c}$ hair follicle. We monitored cell proliferation in control, $scd1^{-/-}$, and $scd1^{-/-c}$ with proliferation markers Ki67 and K17. Highly proliferative Ki67 positive matrix cells with nuclear localization were detected in the hair bulge and bulb of the control and $scd1^{-/-c}$ skin, whereas progenitor cells remained dormant in the $scd1^{-/-}$ skin (Figure 4a–c). Quiescent $scd1^{-/-}$ hair follicles in telogen received signal(s) to start the anagen growth phase with hair formation. Matrix cells surround specialized mesenchymal cells in the dermal papilla to provide a growth stimulus, and differentiate into the central hair shaft, inner root sheath, and companion layer, which guide the shaft to its orifice at the skin surface. The exterior outer root sheath is contiguous with the IFE and contains a reservoir of quiescent stem cells in the bulge.

Cytokeratin K17 is another marker of basal cell differentiation, development, and maintenance of skin appendages, of hair growth follicles, persistence in anagen and of sebaceous glands (Enerback et al., 1997; McGowan and Coulombe, 1998). The reconstituted barrier activated proliferative signals, which induced K17 expression in the hair follicle (Figure 4d).

Western blot of total protein extracts of the control, $scd1^{-/-}$, and $scd1^{-/-c}$ skin revealed very low Ki67 protein expression in control, and increased expression in the $scd1^{-/-}$ and $scd1^{-/-c}$ skin (Figure 4i). This confirmed the strong induction of Ki67 expression by the artificial barrier

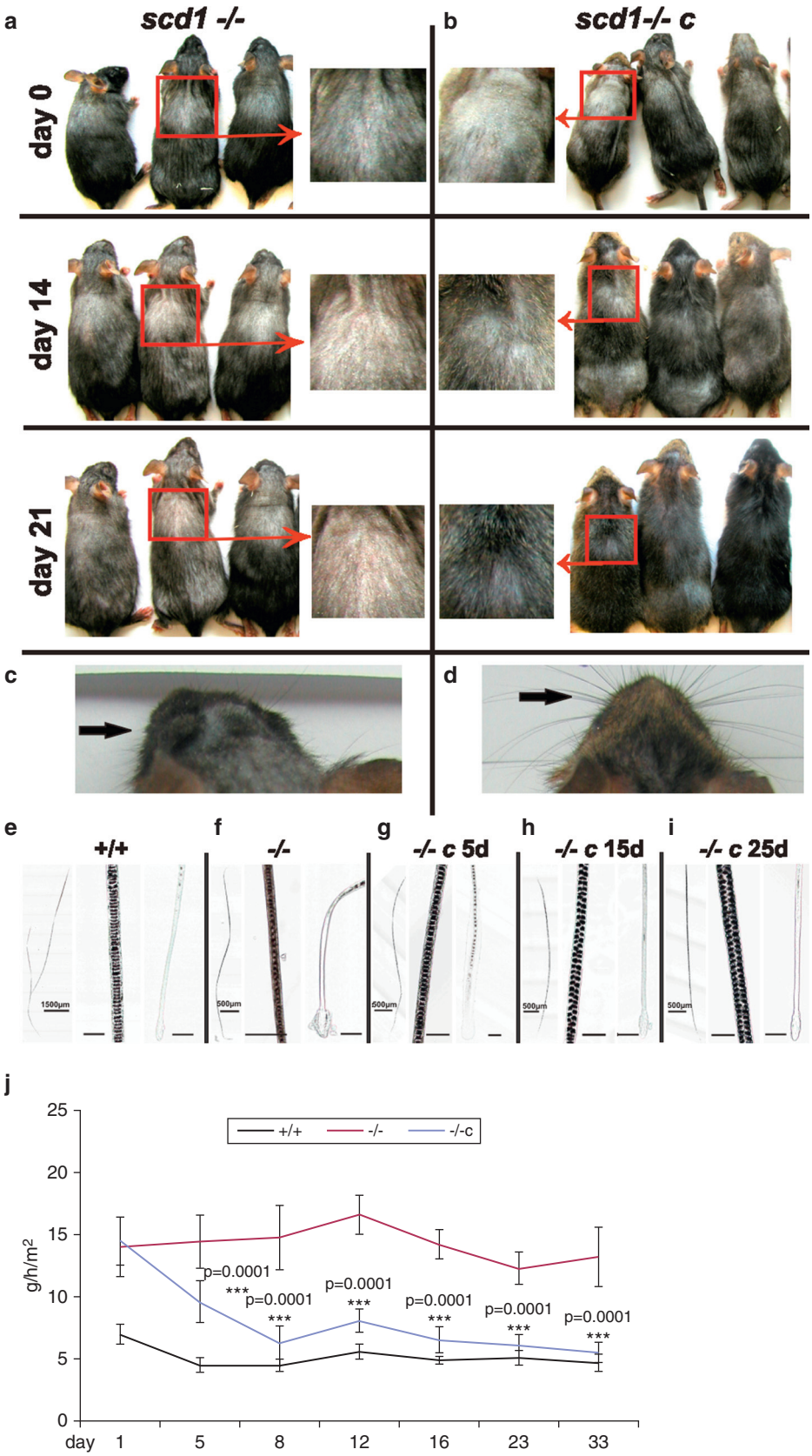

Figure 3. Regular hair growth cycle of adult is rescued in male *scd1*$^{-/-}$ mice by an artificial lipid (paraffin) coat. (**a**) Alopecia in untreated *scd1*$^{-/-}$ mice. (**b**) Follow-up of the hair growth cycle in coated *scd1*$^{-/-c}$ littermates during 3-week maintenance of the artificial barrier at days 0, 14, and 21, showing complete restoration of fur. (**c**) Loss of vibrissae in *scd1*$^{-/-}$ mice and (**d**) regular vibrissae pattern in *scd1*$^{-/-c}$ mice. Comparative hair morphology of isolated hair, hair shafts, and hair bulbs: (**e**) control, (**f**) *scd1*$^{-/-}$ and *scd1*$^{-/-c}$ mice, (**g**) day 5, (**h**) day 15, and (**i**) day 25 after initiation of topical application. (**j**) Transepidermal water loss of cohorts of control, *scd1*$^{-/-}$, and *scd1*$^{-/-c}$ adult mice (n = 8). *P*-values express the significance of differences of *scd1*$^{-/-}$ and *scd1*$^{-/-c}$. Scale bar = 40 μm.

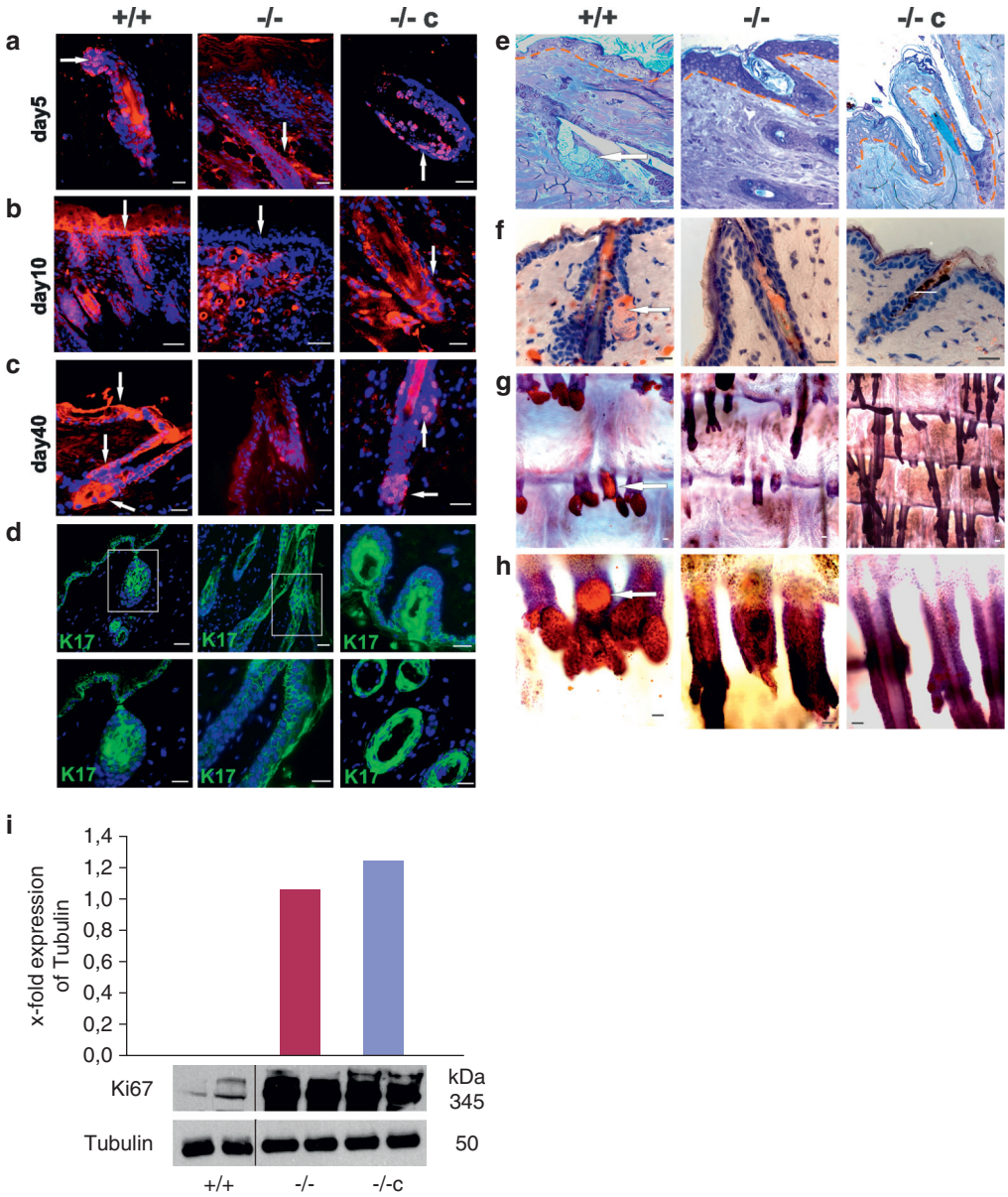

Figure 4. The artificial lipid barrier of *scd1*$^{-/-c}$ adult skin activates epidermal, hair bulge, and bulb progenitor cells, not sebocyte progenitor cells. Paraffin sections of the control, *scd1*$^{-/-}$, and *scd1*$^{-/-c}$ skin were stained with anti-Ki67 antibodies at (**a**) day 5, (**b**) day 10, and (**c**) day 40 after the application of the artificial barrier. Arrows highlight progenitor cells in the epidermis, hair bulge. IHC using (**d**) anti-K17 antibodies. Progenitor sebocytes were not activated by the artificial lipid barrier. (**e**) Ultrathin HE-stained sections and (**f**) oil-red stained sections of the control, *scd1*$^{-/-}$, and *scd1*$^{-/-c}$ adult (8 weeks) skin. (**g, h**) Oil-red stained whole mounts of the control, *scd1*$^{-/-}$, and *scd1*$^{-/-c}$ tail skin, at two magnifications. Densitometry of western blot analyses using (**i**) anti-Ki67 antibodies. Scale bar = 20 μm. HE, hematoxylin and eosin; IHC, immunohistochemistry.

in the *scd1*$^{-/-c}$ skin, shown by immunohistochemistry in Figure 4a–c. However, the western blot analysis of total protein precludes the discrimination between cytosolic and nuclear Ki67.

Progenitor sebocytes remained inactivated and sebaceous glands atrophic

Oil-red stained sections and whole mount preparations of control mice showed regular sebaceous glands, which were missing in the *scd1*$^{-/-}$ and *scd1*$^{-/-c}$ epidermis (Figure 4e–h).

Removal of the artificial coat arrested the hair growth cycle in telogen. Renewal of the artificial barrier activated reservoirs of epidermal multipotent progenitor cells in the bulge and the hair follicle bulb again for reconstitution of the complete hair follicle cycle.

Immunohistochemistry of the epidermis of the *scd1*$^{-/-}$ and *scd1*$^{-/-c}$ skin

We investigated the impact of the artificial barrier on the expression of members of the keratin family in the epidermis of control, *scd1*$^{-/-}$, and *scd1*$^{-/-c}$ mice. Keratins K1 and K10 were expressed in the basal and suprabasal, spinous, and granular epidermal layers, and K5 and anti-K14 antibodies marked the stratum granulosum and keratinosum (Figure 5f–i). Expression of K1 and K10 was restricted to interfollicular basal and suprabasal epidermis cell layers. K5

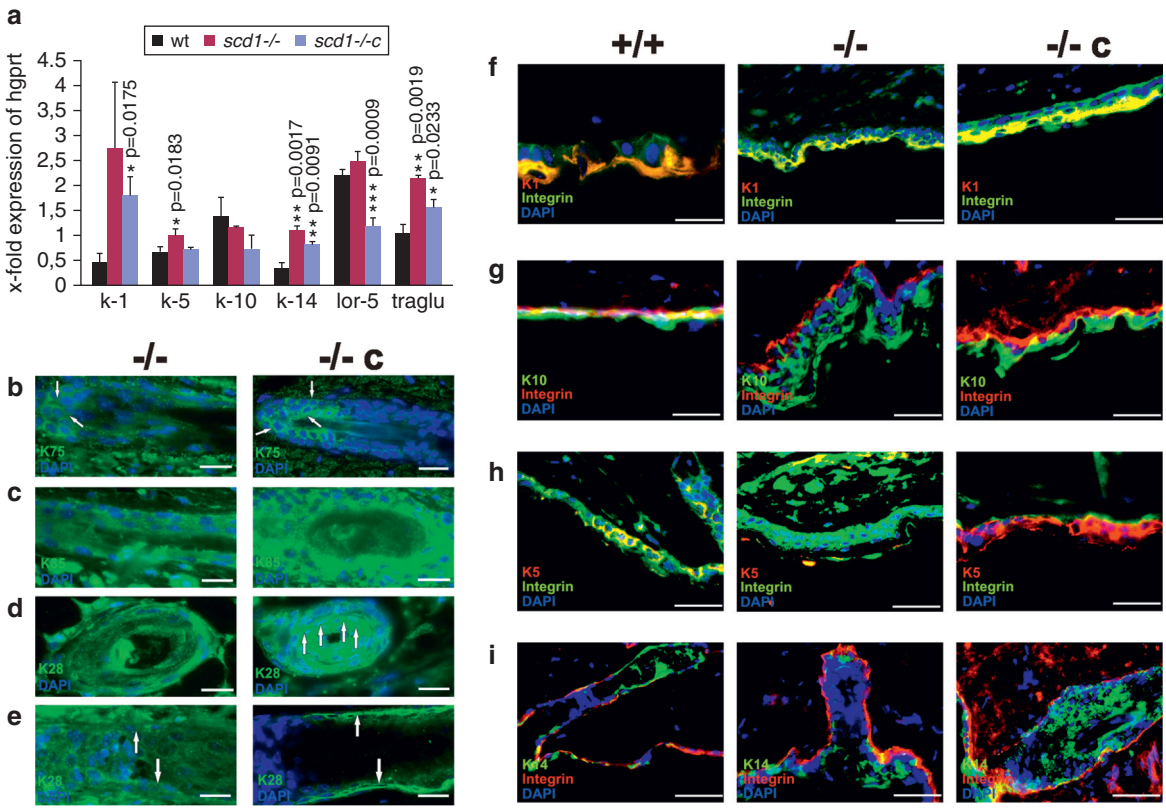

Figure 5. Gene expression of keratins, loricrin, and transglutaminase. (**a**) Real-time PCR *of keratins k-1, k-5, k-10, k-14, loricrin-5 (lor-5),* and *transglutaminase* (*traglu*) in the *control*, $scd1^{-/-}$, and $scd1^{-/-c}$ skin. Mean ± SD. Immunohistochemistry of sections of the skin of control, $scd1^{-/-}$, and $scd1^{-/-c}$ mice, using antibodies recognizing hair follicle epithelium-specific keratins: (**b**) keratin K75, outer root sheath (ORS), and companion layer specific; (**c**) early hair keratin K85 (Hb5) in matrix, cortex, and cuticle, and epithelium; (**d, e**) root sheath-specific K28. Immunohistochemistry of sections of the skin of control, $scd1^{-/-}$, and $scd1^{-/-c}$ mice, using antibodies recognizing (**f**) K1-, (**g**) K10-, (**h**) K5-, and (**i**) K14-specific antibodies. Merged images of sections counterstained with anti-integrin antibody. Scale bars are inserted in images. Scale bar = 20 μm. SD, standard deviation; wt, wild-type.

and K14 in the basal layers are essential for the assembly and organization of barrier structures in the normal stratified epithelium in the control, $scd1^{-/-}$, and $scd1^{-/-c}$ skin.

The structure of the limiting basal membrane underneath the cylindrical cell layer was visualized by heterodimeric integrin α6-ß4, which interacts with extracellular matrix protein laminin5, essential for keratin-specific interaction with the actin cytoskeleton (Supplementary Figure S3 online). Involucrin is synthesized in keratinocytes of the stratum spinosum, and as a highly reactive, soluble cytosolic protein, a glutamyl donor for cross-linking to membrane proteins by transglutaminases. Involucrin and loricrin are the major structures of the insoluble cornified envelope beneath the plasma membrane of terminally differentiated epidermal cells (Hohl et al., 1991); for a review, see Candi et al. (2005).

Reconstitution of hair follicle differentiation in $scd1^{-/-c}$ mice

Next, we compared the hair morphology of $scd1^{-/-}$ and newly formed hair in the $scd1^{-/-c}$ skin by immunohistochemical characterization of the cell layer structure, using early hair keratin type II K85 (Hb5) in the matrix, cortex, and cuticle and late hair keratins by the anti-K28 hair follicle outer root sheath (Schmidt-Ullrich and Paus, 2005). Figure 5b–e revealed the reconstitution of the hair follicle growth cycle and differentiation. K75 (K6hf) and K28 (K25irs4) stained the companion, Henle and Huxley cell layers and the inner root sheath cuticle.

DISCUSSION

This study addresses the currently enigmatic question: how the genetic defect underlying the impaired synthesis of monounsaturated fatty acids causes the dichotomic phenotype, metabolic waste syndrome (anti-obesity), and scarring alopecia in the SCD1-deficient mouse? Here, we describe the impact of the systemic absence of palmitoleic acid (9Z-16:1) on Wnt3a/ß-catenin signaling in SCD1-deficient epidermis and appendages.

Meticulous studies have unveiled the central role of the canonical Wnt/ß-catenin signaling pathway in skin barrier homeostasis, hair follicle growth cycle, morphogenesis, and follicle regeneration and the maintenance of sebaceous glands (Lim and Nusse, 2013). Wnt-signaling requires O-palmitoleoylation of Wnt proteins for intracellular transport to lipid rafts in the plasma membrane and secretion (Takada et al., 2006).

The lack of palmitoleoyl-CoA in $scd1^{-/-}$ mice prohibits O-acylation of Wnt3a by membrane-bound O-acyltransferase, the essential step for the activation of Wnt3a/ß-catenin signaling and activation of transcription factor Lef1. Lef1 is required for the lineage development of keratinocytes, hair follicle, and sebocytes and the assembly of the epidermal

barrier (DasGupta and Fuchs, 1999; Niemann and Watt, 2002).

Deviating from the canonical Wnt/ß-catenin signaling pathway, 16:1 deficiency caused *Wnt3a* suppression (3×), left *ß-catenin* expression unchanged, overexpression of *mboat (porc)* expression (3×), and overexpression of *lef1* (>10×) in the *scd1*$^{-/-}$ and *scd1*$^{-/-c}$ skin. The artificial barrier did not improve the 3-fold and 2-fold suppressed steady-state RNA expression of 18:0- and 16:0-specific ceramide synthases CerS1 and Cers5 in the *scd1*$^{-/-}$ skin. Altered expression of lipid modifying enzymes in the skin of mutant Lef1, for example, SCD1 and Cers3, has led to the conclusion that Lef1 regulates the lipid barrier function (Fehrenschild et al., 2012).

Hormone like or "lipokine" functions have been assigned to palmitoleate (16:1), synthesized in WAT, the site of de novo lipogenesis. 16:1 is released from adipocytes and systemically distributed by fatty acid binding proteins as chaperone carriers, which link alterations of WAT and the regulation of systemic metabolic homeostasis. Acting as "insulin sensitizing hormone," 16:1 is supposed to improve glucose metabolism and prevents hepatosteatosis (Cao et al., 2008). Subsequent studies have questioned this role of 16:1 as lipokine (Guo et al., 2012).

The systemic absence of palmitoleate in the *scd1-null* mouse, shown in this study, provides no evidence for a systemic lipokine function of palmitoleate. The artificial lipid barrier was able to normalize the metabolic parameters in the absence of palmitoleate in the *scd1*$^{-/-}$ skin. Fasting glucose levels were similar and fasting insulin levels slightly higher compared with control mice. Glucose and insulin tolerance tests in *scd1*$^{-/-}$ mice on chow diet elicited minor, but significantly elevated insulin resistance, which support those of previously reported studies (for a review, see Hsu et al., 2014). The analysis of total liver lipids as well as the histology of oil-red stained liver sections of *scd1*$^{-/-}$ and control mice precludes hepatosteatosis (Supplementary Figure S2 online).

Artificial lipid barrier induces the regular hair growth cycle in the *scd1*$^{-/-}$ skin

Wnt signaling and ß-catenin stabilization has been demonstrated to transiently activate the Lef1/Tcf complex and specify the differentiation of lineages of the newly developing hair follicle, IFE, and sebocytes. ß-Catenin-induced lineage conversion in the adult epidermis of transgenic has been demonstrated in ΔNß-catenin-endoplasmic reticulum mice (N-terminally truncated, ß-catenin fused to the ligand-binding domain of a mutant estrogen receptor) (Lo Celso et al., 2004). Topical application of 4-hydroxytamoxifen induced ß-catenin activity, which recruited the growth cycle of resting hair follicles from IFE and reprogramming sebaceous glands, but left the interfollicular epidermal differentiation unaffected.

Bulge stem cells have been shown to maintain epidermis and both appendages, hair follicle and sebaceous glands (Cotsarelis, 2006; Morris et al., 2004; Tumbar et al., 2004). Other experiments refer to bulge cells maintaining homeostasis of hair follicles and sebaceous glands only, not of epidermis. No renewal of sebaceous glands from hair follicle stem cells has been observed (Niemann and Watt, 2002). The activation of hair bulge progenitor cells without activation of progenitor sebocytes, observed here, is at variance with this proposal. On application of the artificial epidermal lipid barrier, surprisingly, Ki67 marker positive progenitor cells with different cell responsiveness proliferated and egressed from the bulge niche and feed into the epidermal compartment and the hair follicle in the *scd1*$^{-/-c}$ epidermis.

The hair morphology of control and *scd1*$^{-/-c}$ showed similar appearance during the growth cycle at days 5, 15, and 25, unlike *scd1*$^{-/-}$ mice, halted in telogen (Figure 3e–i).

Sebocyte progenitor cells, however, were not activated and sebaceous glands not reconstituted (Figure 4). This observation strengthens the notion of different subsets of progenitor cells for epidermis, hair, and sebaceous glands.

Noncanonical Wnt independent regulation of ß-catenin stability and of Lef1 coactivation, as well as ß-catenin independent mechanisms associated with Wnt signaling and Lef1 transcriptional activation has been described in several signaling pathways (Lim and Nusse, 2013).

The artificial barrier neither changed the expression of genes of the Wnt3a/ß-catenin pathway nor of specific keratins significantly in the *scd1*$^{-/-}$ skin, for example, of spinous and granular epidermal cell markers K1 and K10, stratum granulosum, and keratinosum markers K5 and K14, and of loricrin as a marker of the granular cell layer in the IFE of control. *K17* is an early gene, the *lef1*-driven expression of which has direct implications for the morphogenesis of skin epithelia and ectoderm-derived appendages, hair follicle, and sebaceous glands in adult mice (McGowan and Coulombe, 1998). The enhanced expression of both *lef1* and *k17* in the epidermis and hair follicle cell layers of the adult *scd1*$^{-/-c}$ skin induced the formation of multiple placodes, but had no influence on precursor sebocytes (Figure 4).

The expression of BMP inhibitors, key markers of pathways active in telogen, of Noggin and Wnt in the telogen-anagen transition, and of Shh in early anagen was strongly downregulated in the *scd1*$^{-/-}$ and *scd1*$^{-/-c}$ skin and not rescued by the artificial lipid coat (Figure 2).

The artificial barrier also activated melanocyte progenitor cells in the bulge of *scd1*$^{-/-c}$ mice indicated by the C57Bl/6-fur color (Figure 3).

Reconstitution of the complete hair growth cycle in *scd1*$^{-/-}$ mice in the absence of sebaceous glands, reported here, precludes the proposal derived from the autosomal recessive SCD1-deficient asebiaJ and 2J mutants, which holds the absence of sebaceous glands in these mutants liable for the inhibition of the slipping of the hair shaft out of the inner root sheath, and development of scaring alopecia (Sundberg et al., 2000). Loricrin- and involucrin-expression remained unchanged in the stratum corneum under the artificial lipid barrier (Supplementary Figure S3 online).

Future experiments will address the link between the physical properties of the artificial epidermal barrier regulating TEWL and thermogenesis in *scd1*$^{-/-c}$ skin and signaling pathways underlying the selectivity in skin progenitor cell lineage decision in either reprogramming stem cells or retained plasticity of progenitor cells.

The readily reversible telogen-anagen reentry and exit in the *scd1*$^{-/-}$ mouse in response to the application or removal

of the artificial lipid barrier provides an unbiased model for further exploring the molecular link between the physical properties of the epidermal barrier and the selectivity in skin progenitor cell lineage decision. The mutant might be useful in disclosing molecular events underlying human scarring alopecia and other skin diseases. Furthermore, this genetically well-defined in vivo model might be intriguingly helpful in studies of the regulation of the hair growth cycle, which is inducible ad libitum in the same animal by the simple application of an artificial lipid barrier. The unbiased genotype and phenotype of the *scd1*$^{-/-}$ mice and the noninvasive experimental conditions in this study help to reduce the number of animals needed for statistically secured experiments.

MATERIALS AND METHODS

Scd1$^{-/-}$ mouse mutant

Generation and genetic characterization of the *scd1*$^{-/-}$ mouse has been described (Binczek et al., 2007). *Scd1*$^{-/-}$ mice have been back-crossed and are maintained on a C57BL/6N background. Animal studies were approved by the Institutional Animal Care and Use Committee of the University of Cologne and the Governmental authority.

Application of the artificial lipid barrier

Mice were single-housed. For the application of the artificial lipid coat, the mouse was placed on the cover grid of the cage and lubricated evenly from the head to tail with approximately 500 mg inert Vaseline/mouse (Vaseline, weiß, Ph.Eur. Hautschutzsalbe, Art.Nr.80048101, PZN 04377121, EAN 4034671000103, Bombastus Werke AG, Freital, Germany), at intervals of 2 days. The bottom of the cage was covered with fibrous web (Sandler AG, Schwarzenbach/Saale, Germany) for dust free bedding.

Real-time PCR

RNA was isolated for real-time PCR from control and *scd1*$^{-/-}$ using Trizol (Invitrogen, Karlsruhe, Germany), reverse-transcribed using a transcriptase kit (Life Technologies, Darmstadt, Germany). Quantitative PCR reactions were performed with the ABI Prism 7900HT employing a 96-well format, the Fast SYBR Green Master Mix (Applied Biosystems, Darmstadt, Germany), following the manufacturer's protocol.

Lipidomic analysis

Isolation, separation, identification, and quantification were performed as described previously (Stoffel et al., 2014).

Histology and immunohistochemistry

Mice were perfused from the left ventricle, the right atrium opened, with 20 ml saline, followed by 50 ml 4% phosphate buffered paraformaldehyde. Tissues were fixed in the same buffer overnight at 4 °C, dehydrated, and embedded for cryo- and paraffin-sections. Sections (5 μm) were deparaffinized, rehydrated, permeabilized in 0.2% Triton X-100 for 10 minutes and blocked with 4% normal goat serum for 30 minutes and immunostained as described before (Binczek et al., 2007). Whole mount preparations were used for oil-red and immunostaining as described (Braun et al., 2003). Hair morphology was documented by the Slidescanner Leica SCN400 (Fa. Leitz, Wetzlar, Germany).

Protein analysis by western blotting

Protein aliquots were analyzed by western blot hybridization, using the following antibodies: ß-catenin (BD Biosciences, Heidelberg, Germany), Wnt3a, Scd1, and Noggin (Santa Cruz, Heidelberg, Germany), occludin (Zymed Lab., San Francisco), ZO1 (Invitrogen), Lef1, Ki67, and Shh, (abcam, Cambridge), and tubulin (Sigma, Missouri). Western blots were quantified by densitometry using the NIH IMAGE J2X program.

Enzyme assay

Palmitoyl-CoA desaturase activity in the microsomal fraction of the control and *scd1*$^{-/-}$ liver was measured by the enzymatic assay described in the Supplementary Material online.

Statistical analysis

Results are expressed as mean ± standard deviation. Statistical significance of differences between two groups was determined by a two-tailed Student's test using GraphPad QuickCalcs: *t*-test calculator. *P*-values of ≤ 0.05*, ≤ 0.01**, and ≤ 0.001*** were considered significant.

CONFLICT OF INTEREST

The authors state no conflict of interest.

ACKNOWLEDGMENTS

This project has been generously supported by the CMMC (Center of Molecular Medicine Cologne) and CECAD (Cluster of Excellence, Cellular Stress Response in Aging Related Diseases), University of Cologne, 50931 Cologne, Germany. The support by Dr Mahabir-Brenner, Animal Facilities, CMMC Cologne, is gratefully acknowledged. We thank Prof Thomas Krieg, Department of Dermatology, University of Cologne, Germany, for revising the manuscript.

SUPPLEMENTARY MATERIAL

Supplementary material is linked to the online version of the paper at www.jidonline.org, and at http://dx.doi.org/10.1016/j.jid.2017.02.973.

REFERENCES

Alonso L, Fuchs E. Stem cells of the skin epithelium. Proc Natl Acad Sci USA 2003;100(Suppl. 1):11830–5.

Andl T, Reddy ST, Gaddapara T, Millar SE. WNT signals are required for the initiation of hair follicle development. Dev Cell 2002;2:643–53.

Binczek E, Jenke B, Holz B, Gunter RH, Thevis M, Stoffel W. Obesity resistance of the stearoyl-CoA desaturase-deficient (scd1$^{-/-}$) mouse results from disruption of the epidermal lipid barrier and adaptive thermoregulation. Biol Chem 2007;388:405–18.

Braun KM, Niemann C, Jensen UB, Sundberg JP, Silva-Vargas V, Watt FM. Manipulation of stem cell proliferation and lineage commitment: visualisation of label-retaining cells in wholemounts of mouse epidermis. Development 2003;130:5241–55.

Candi E, Schmidt R, Melino G. The cornified envelope: a model of cell death in the skin. Nat Rev Mol Cell Biol 2005;6:328–40.

Cao H, Gerhold K, Mayers JR, Wiest MM, Watkins SM, Hotamisligil GS. Identification of a lipokine, a lipid hormone linking adipose tissue to systemic metabolism. Cell 2008;134:933–44.

Cohen P, Miyazaki M, Socci ND, Hagge-Greenberg A, Liedtke W, Soukas AA, et al. Role for stearoyl-CoA desaturase-1 in leptin-mediated weight loss. Science 2002;297:240–3.

Cotsarelis G. Epithelial stem cells: a folliculocentric view. J Invest Dermatol 2006;126:1459–68.

DasGupta R, Fuchs E. Multiple roles for activated LEF/TCF transcription complexes during hair follicle development and differentiation. Development 1999;126:4557–68.

Enerback S, Jacobsson A, Simpson EM, Guerra C, Yamashita H, Harper ME, et al. Mice lacking mitochondrial uncoupling protein are cold-sensitive but not obese. Nature 1997;387:90–4.

Fehrenschild D, Galli U, Breiden B, Bloch W, Schettina P, Brodesser S, et al. TCF/Lef1-mediated control of lipid metabolism regulates skin barrier function. J Invest Dermatol 2012;132:337–45.

Guo X, Li H, Xu H, Halim V, Zhang W, Wang H, et al. Palmitoleate induces hepatic steatosis but suppresses liver inflammatory response in mice. PLoS One 2012;7:e39286.

Hofmann K. A superfamily of membrane-bound O-acyltransferases with implications for wnt signaling. Trends Biochem Sci 2000;25:111–2.

Hohl D, Mehrel T, Lichti U, Turner ML, Roop DR, Steinert PM. Characterization of human loricrin. Structure and function of a new class of epidermal cell envelope proteins. J Biol Chem 1991;266:6626–36.

Hsu YC, Li L, Fuchs E. Emerging interactions between skin stem cells and their niches. Nat Med 2014;20:847–56.

Huelsken J, Birchmeier W. New aspects of Wnt signaling pathways in higher vertebrates. Curr Opin Genet Dev 2001;11:547–53.

Lim X, Nusse R. Wnt signaling in skin development, homeostasis, and disease. Cold Spring Harb Perspect Biol 2013;5:a008029.

Lo Celso C, Prowse DM, Watt FM. Transient activation of beta-catenin signalling in adult mouse epidermis is sufficient to induce new hair follicles but continuous activation is required to maintain hair follicle tumours. Development 2004;131:1787–99.

Lowry WE, Blanpain C, Nowak JA, Guasch G, Lewis L, Fuchs E. Defining the impact of beta-catenin/Tcf transactivation on epithelial stem cells. Genes Dev 2005;19:1596–611.

McGowan KM, Coulombe PA. Onset of keratin 17 expression coincides with the definition of major epithelial lineages during skin development. J Cell Biol 1998;143:469–86.

Miyazaki M, Bruggink SM, Ntambi JM. Identification of mouse palmitoyl-coenzyme A Delta9-desaturase. J Lipid Res 2006;47:700–4.

Miyazaki M, Man WC, Ntambi JM. Targeted disruption of stearoyl-CoA desaturase1 gene in mice causes atrophy of sebaceous and meibomian glands and depletion of wax esters in the eyelid. J Nutr 2001;131:2260–8.

Morris RJ, Liu Y, Marles L, Yang Z, Trempus C, Li S, et al. Capturing and profiling adult hair follicle stem cells. Nat Biotechnol 2004;22:411–7.

Niemann C, Watt FM. Designer skin: lineage commitment in postnatal epidermis. Trends Cell Biol 2002;12:185–92.

Ntambi JM, Miyazaki M. Recent insights into stearoyl-CoA desaturase-1. Curr Opin Lipidol 2003;14:255–61.

Nusse R. Wnts and Hedgehogs: lipid-modified proteins and similarities in signaling mechanisms at the cell surface. Development 2003;130:5297–305.

Sampath H, Flowers MT, Liu X, Paton CM, Sullivan R, Chu K, et al. Skin-specific deletion of stearoyl-CoA desaturase-1 alters skin lipid composition and protects mice from high fat diet-induced obesity. J Biol Chem 2009;284:19961–73.

Schmidt-Ullrich R, Paus R. Molecular principles of hair follicle induction and morphogenesis. BioEssays: news and reviews in molecular, cellular and developmental biology 2005;27:247–61.

Stoffel W, Hammels I, Jenke B, Binczek E, Schmidt-Soltau I, Brodesser S, et al. Obesity resistance and deregulation of lipogenesis in Delta6-fatty acid desaturase (FADS2) deficiency. EMBO Rep 2014;15:110–20.

Sundberg JP, Boggess D, Sundberg BA, Eilertsen K, Parimoo S, Filippi M, et al. Asebia-2J (Scd1(ab2J)): a new allele and a model for scarring alopecia. Am J Pathol 2000;156:2067–75.

Takada R, Satomi Y, Kurata T, Ueno N, Norioka S, Kondoh H, et al. Monounsaturated fatty acid modification of Wnt protein: its role in Wnt secretion. Dev Cell 2006;11:791–801.

Tumbar T, Guasch G, Greco V, Blanpain C, Lowry WE, Rendl M, et al. Defining the epithelial stem cell niche in skin. Science 2004;303:359–63.

Willert K, Brown JD, Danenberg E, Duncan AW, Weissman IL, Reya T, et al. Wnt proteins are lipid-modified and can act as stem cell growth factors. Nature 2003;423:448–52.

Zhai L, Chaturvedi D, Cumberledge S. Drosophila wnt-1 undergoes a hydrophobic modification and is targeted to lipid rafts, a process that requires porcupine. J Biol Chem 2004;279:33220–7.

Zheng Y, Prouty SM, Harmon A, Sundberg JP, Stenn KS, Parimoo S. Scd3—a novel gene of the stearoyl-CoA desaturase family with restricted expression in skin. Genomics 2001;71:182–91.